Journal of Power Sources 195 (2010) 7765–7769

Contents lists available at ScienceDirect

Journal of Power Sources

journal homepage: www.elsevier.com/locate/jpowsour

Short communication

PBI-based composite membranes for polymer fuel cells

V. Kurdakova [a,*], E. Quartarone [a], P. Mustarelli [a,*], A. Magistris [a], E. Caponetti [b], M.L. Saladino [b]

[a] Dipartimento di Chimica Fisica "M. Rolla" and INSTM, Università di Pavia, Via Taramelli 16, 27100 Pavia, Italy
[b] Dipartimento di Chimica Fisica "Filippo Accascina", Università di Palermo, Viale Delle Scienze, Parco d'Orleans 2, 90128 Palermo, Italy

ARTICLE INFO

Article history:
Received 30 July 2009
Received in revised form
18 September 2009
Accepted 30 September 2009
Available online 7 October 2009

Keywords:
Proton exchange membrane
PBI
Electrochemical Impedance Spectroscopy

ABSTRACT

In the present study poly(2,2-(2,6-pyridin)-5,5-bibenzimidazole) was used for the preparation of novel MEAs for high-temperature polymer fuel cells (HT-PEMFCs). We prepared hybrid materials with two types of silica fillers in order to increase the MEA performances using this polymer. The membranes were characterized in terms of their microstructure and thermal stability. Cell operation tests and Electrochemical Impedance Spectroscopy were used for the characterization of the MEAs. A maximum power density of about 80 mW cm^{-2} was obtained at 300 mA cm^{-2} by using an imidazole-modified silica filler. The EIS technique showed that the fillers chiefly help to reduce the charge transfer resistance of the cathodic side. The gas transfer resistance may be neglected with respect to R_{ct}, at least at low current densities.

1. Introduction

High-temperature operated PEMFCs have attracted substantial attention in the last decade due to their wide applicability, the possibility to reduce costs of the existing devices and to make them more environmentally friendly. In order to optimize the fuel cell performances a lot of work has been focused on material development. Among the polymers of choice, acid-doped polybenzimidazoles seem to offer an optimal combination of properties such as mechanical stability, higher values of conductivity and the tolerance towards fuel impurities at temperatures up to 200 °C. Li et al. [1] have recently reviewed the studies devoted to the development of PBI-based polymers, including monomer synthesis, membrane casting, physical–chemical characterizations and applications to fuel cell technologies. Hu et al. [2] performed long durability tests and showed that at 150 °C after 100 h activation, the cell performance began to degrade with rate 150 μV h^{-1} at 640 mA cm^{-2}. At present, the main problems associated with polybenzimidazole PEMFCs are seem to be acid leaching and catalyst degradation processes which dramatically decrease the fuel cell performances. [3] On the other hand, it has been recently reported that during the operation at 160 °C the acid loss could not be the major factor of the fuel cell failure [4].

In order to improve functional properties of the membranes, one of the main directions in the design of PBI-based materials is to combine the organic matrix with an inorganic material. PBI composites with inorganic proton conductors including zirconium phosphate (ZrP), (Zr(HPO$_4$)2$^-$$nH_2$O), phosphotungstic acid and silicotungstic acid were prepared by Bjerrum and co-workers [5]. Chuang et al. fabricated nanocomposites with PBI and an organically modified montmorillonite (m-MMT) [6]. They showed that both the mechanical properties (thermal expansion, tensile modulus) and the methanol barrier ability were significantly improved by the addition of m-MMT. Li et al. [7] fabricated composite PBI membranes with $Cs_{2.5}H_{0.5}PMo_{12}O_{40}$ (CsPOM). NMR results indicated possible formation of chemical bonds between CsPOM and PBI. Jang and Yamazaki [8] synthesized zirconium tricarboxybutylphosphonate (Zr(PBTC)) particles embedded in PBI. It was pointed out that such additives improve proton conductivity due to a number of hydrogen bonds among the COOH, PBI, and water molecules in Zr(PBTC)/PBI membranes. Conductivity values with 50 wt.% Zr(PBTC) were 3.82×10^{-3} S cm^{-1} at 200 °C. Sulfonated silica nanoparticles were used as dopants to prepare PBI composite membranes for PEMFCs [9]. According to the reported results, sulfonic groups enhanced compatibility between silica nanoparticles and organic matrices. Integration of sulfonated silica nanoparticles to PBI membranes also depressed the methanol permeability.

In a previous work we reported the physical–chemical and transport properties of poly(2,2-(2,6-pyridin)-5,5-bibenzimidazole) (PBI-5N) composite membranes containing two different fillers: a mesostructured silica (SBA-15), and a sol–gel SiO2 with imidazole groups (SiO_2-Im) [10]. We showed that the imidazole-based filler is more effective than mesostructured silica in improving the conductivity of the membrane after acid leaching.

In this study we extended our interest to the investigation of the functional properties of MEAs based on PBI-5N composite membranes. We used mesoporous silica MCM-41 and the

* Corresponding authors. Tel.: +39 0382987205; fax: +39 0382987776.
E-mail addresses: val.kurdakova@gmail.com (V. Kurdakova), piercarlo.mustarelli@unipv.it (P. Mustarelli).

0378-7753/$ – see front matter © 2009 Elsevier B.V. All rights reserved.
doi:10.1016/j.jpowsour.2009.09.064

imidazole-based silica as promising candidates to improve the MEA properties for fuel cell applications. *I–V* polarization curves and, Electrochemical Impedance Spectroscopy were used to study the role played by silica fillers in the fuel cell operation.

2. Experimental

2.1. Membrane preparation

The procedure for the poly(2,2-(2,6-pyridin)-5,5-bibenzimidazole) powder synthesis is reported in [11]. The average molecular weight was 16377 g mol^{-1}. The PBI-5N membranes were prepared by a standard solvent casting method. Monomers (5 wt.%) were dissolved in N,N-dimethylacetamide at 60 °C. Subsequently, proper amounts of the fillers (from 5 wt.% to 20 wt.%) were dispersed by sonication in the polymer solution, which was then cast in order to obtain membranes with the thickness in a range of 95–100 μm. Then composite membranes were activated by immersion in an aqueous solution of phosphoric acid (75 wt.%) at room temperature for 96 h and then dried at 200 °C to constant weight.

Two types of SiO_2-based fillers were used in our work: (a) silica, functionalized with imidazole groups (SiO_2-Im) and (b) mesoporous silica, MCM-41.

SiO_2-Im filler was synthesized in our laboratory through a sol–gel route [12]. Its specific surface area was 3.5 m^2 g^{-1} according to BET analysis. Mesoporous silica, MCM-41, is provided by our colleagues of University of Palermo. The synthetic route is reported in [13]. The specific surface area of MCM-41 was about 930 m^2 g^{-1} and the pore diameter around 40 Å.

The membrane electrode assembly was made with HT140EW gas-diffusion layers (E-TEK). The catalyst was carbon-platinum powder with 30 wt.% Pt, so the Pt loading was 0.5 mg cm^{-2} both for anodic and cathode sizes. MEA was pressed at 120 °C for 10 min at the pressure of 1 ton. The active cell area was 5 cm^2.

2.2. Characterization

Scanning electron microscopy images were collected in low vacuum mode by using a Scanning Electron Microscope VEGA TS 5136 (Vega-Tescan) with accelerating voltage of 30 kV. The surfaces of samples were sputtered with gold.

The TGA scans were recorded at 5 °C min^{-1} under nitrogen flow with a 2950 TGA (TA Instruments).

The electrochemical measurements were performed with a BT-552 Membrane Conductivity and Single Cell Fuel Cell Test System (BekkTech LLC) in temperature range 100–150 °C. The cell operated at ambient pressure and without humidification of feed gas steams. The hydrogen flow rate was 0.07 L min^{-1} and the air flow rate was 0.30 L min^{-1}.

The impedance spectroscopy measurements were performed at 150 °C with a frequency response analyzer (FRA Solartron 1255) connected to an electrochemical interface (Solartron 1287), in the frequency range 5 MHz to 0.1 Hz and a voltage amplitude of 50 mV. The impedance spectra were fitted with the ZView 3.0a program (Scribner Associates Inc.).

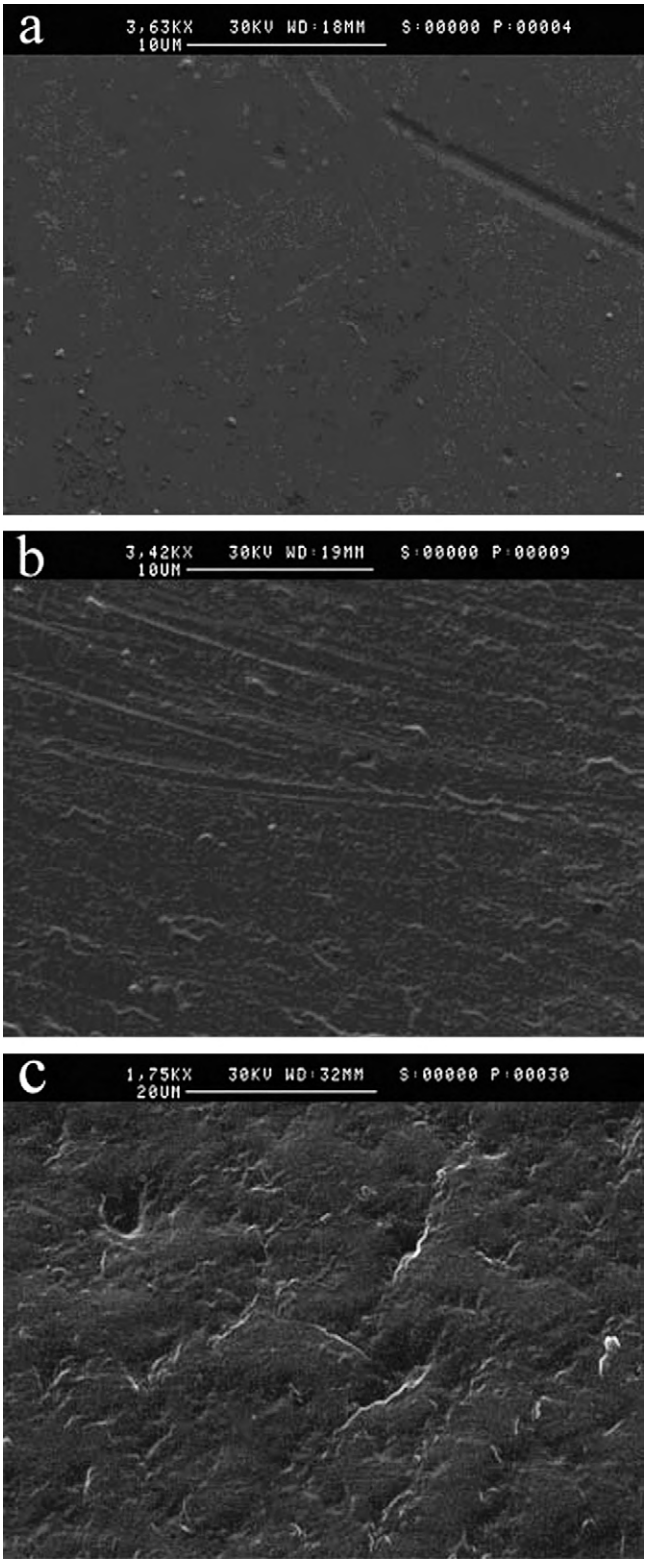

Fig. 1. SEM pictures for: (a) H_3PO_4/PBI-5N membrane, (b) H_3PO_4/PBI-5N composite membrane with (20 wt.%) SiO_2-Im, (c) H_3PO_4/PBI-5N composite membrane with (5 wt.%) MCM-41 mesoporous silica.

3. Results and discussion

3.1. Membrane microstructure

The surface microstructures of some selected membranes are presented in Fig. 1. The pure polymer shows a smooth surface. The addition of imidazole-functionalized silica does not change considerably the surface microstructure of the membrane. Probably, the presence of imidazole group facilitated a homogeneous distribution of the silica filler in the membrane and prevented agglomeration processes. In the case of mesoporous silica, higher surface roughness of the membrane was detected by SEM. The best results in terms of filler distribution homogeneity were obtained in a case of usage of 5 wt.% of MCM-41 and 15–20 wt.% of imidazole containing

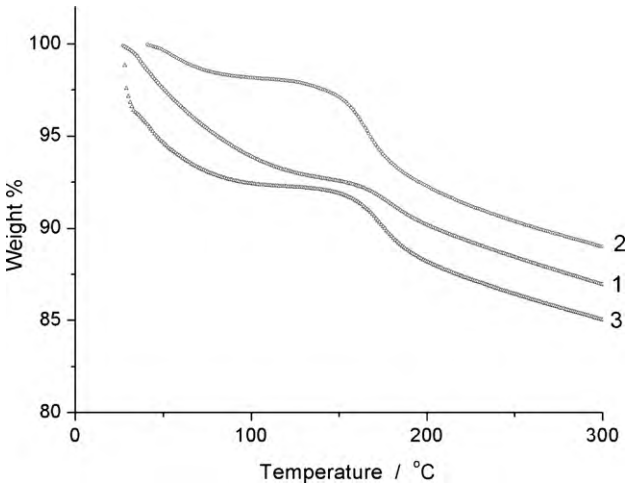

Fig. 2. TGA plots of different acid-doped PBI-5N composite membranes: 1—PBI-5N membrane, 2—containing 5 wt.% of MCM-41 silica, and 3—containing 20 wt.% SiO_2-Im.

silica. The obtained images indicated homogeneous distribution of the silica component inside H_3PO_4/PBI-5N activated membranes.

3.2. Thermal stability of the membranes

The thermogravimetric analysis of the pure membrane and the composite materials are presented below (Fig. 2). It is clearly seen that all the membranes undergo a progressive weight loss up to 100 °C and it can be attributed to the water evaporation process. Between 100 °C and 150 °C there is a stability plateau whose width is increased with the addition of both fillers. A second decomposition step begins at temperatures higher than 160 °C as a result of the polycondensation reactions of the phosphoric acid [14]. All the electrochemical experiments were performed within the temperature range of the thermal stability of the membranes. A complete physical–chemical and transport analysis of pure PBI-5N membranes and of those with SiO_2-Im filler is reported in [10,11]. In terms of the thermal and transport properties MCM-41 is similar to SBA-15. In our paper we will focus our attention only on the effect of the fillers on the electrochemical properties of the MEAs.

3.3. Polarization behavior of the PEMFC

The fuel cell performances of the H_3PO_4/PBI-5N composite membranes are presented in Fig. 3a and b. The polarization curves were obtained in the temperature range 100–150 °C with constant gas flow rates (H_2 0.07 L min^{-1} and air 0.3 L min^{-1}) in conditions of low humidity (<1%). Polarization curves revealed mainly two parts: a voltage drop in the region of low current density and *I–V* linear dependence due to the ohmic resistance of the cell in the range of high current density. It was reported that in the region of higher current densities the electrode behavior is controlled by mass transport diffusion processes [15]. Mass transport limitations probably depend on gas flow rate and gas backing porosity and water management [16]. All the studied MEAs were characterized by good OCV reproducibility in time. The MEAs fabricated with the pure H_3PO_4/PBI-5N membrane displayed lower values of OCV (about 600 mV), in comparison with those based on the composite materials. That result may be linked to the ability of the used silica fillers to increase the local proton concentration within PBI-5N membranes, at least in the case of SiO_2-Im filler. On the other hand, the presence of silica can reduce the H_2 permeation, so increasing the OCV. The MEA containing the SiO_2-Im filler provided a more extended linear region of ohmic resistance in comparison with

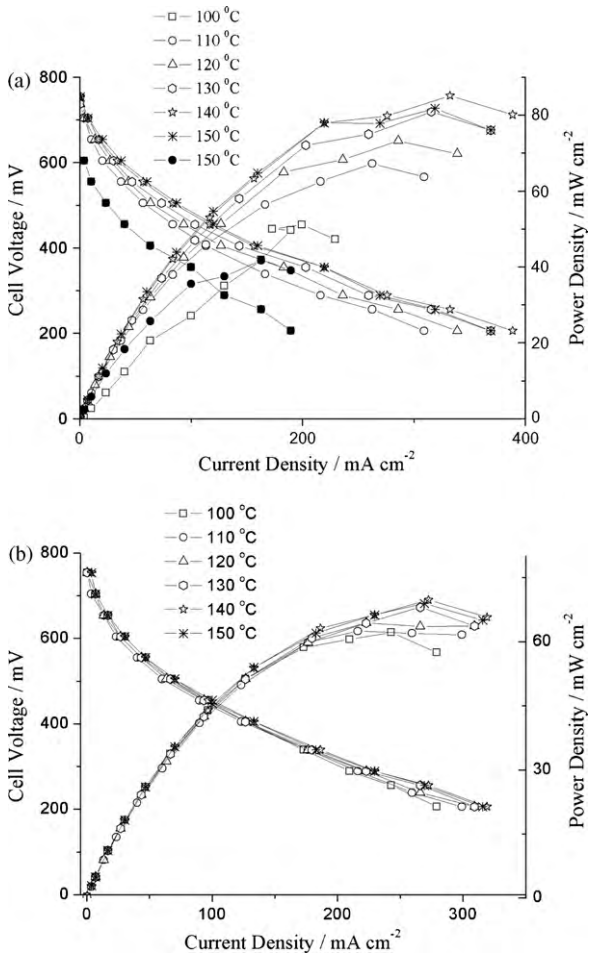

Fig. 3. Polarization curves obtained at ambient pressure, H_2/air constant flow rate gases, without humidity and at different temperatures. (a) H_3PO_4/PBI-5N composite membrane with 20 wt.% SiO_2-Im; solid symbols corresponded to the curves for the pure H_3PO_4/PBI-5N membrane, and (b) H_3PO_4/PBI-5N composite membrane with 5 wt.% MCM-41 mesoporous silica.

the other materials used in our experiments. This MEA also gave a maximum power density about 20% higher than that provided by MCM-41 (83 mW cm^{-2} vs. 70 mW cm^{-2}).

Another interesting difference between two fillers can be observed by comparison of the polarization curves derived at different temperatures. In the case of the membranes with SiO_2-Im filler the MEA performances were dependent on the cell temperature. The non-linear behavior was observed since the maximum power density was obtained at 140 °C instead that at 150 °C. In contrast, the behavior of the MEA with MCM-41 silica was nearly independent on the cell temperature except the highest currents region. The power density values at low temperature for those membrane electrode assembling were higher in absolute values in comparison with SiO_2-Im based MEA. A possible explanation of that effect could be found in a nature of MCM-41. In fact, thanks to the large surface area and the mesoporous structure, this filler is capable of retaining more water molecules which can efficiently contribute to the proton transport. This contribution becomes less relevant above 120–130 °C, because of the water evaporation, as confirmed by the larger loss slope showed by TGA (see Fig. 2).

3.4. Electrochemical Impedance Spectroscopy (EIS)

Electrochemical Impedance Spectroscopy is a useful technique for the characterization of interfacial and bulk materials properties.

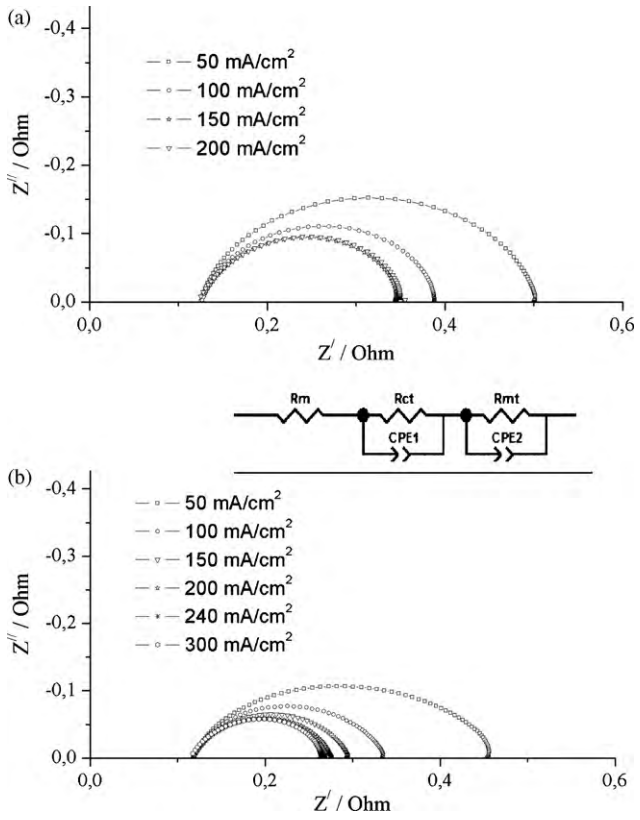

Fig. 4. Nyquist presentation of impedance spectra, measured at different current densities, *t* cell = 150 °C, at ambient pressure, H_2/air constant flow rate gases, 0% RH (a) H_3PO_4/PBI-5N membrane, (b) H_3PO_4/PBI-5N composite membrane with 20 wt.% SiO_2-Im. The upper insert is an equivalent scheme for PEM fuel cell.

In Fig. 4 some selected Nyquist plots are reported for H_3PO_4/PBI-5N and H_3PO_4/PBI-5N with SiO_2-Im MEAs under fuel cell operation at different current densities. Before each impedance measurement, we kept the cell under the given current density at least for 10 min, in order to reach steady-state operation conditions. In the whole range of the explored current densities, the impedance diagrams were made by only one depressed semicircle. In principle, this relaxation can be attributed both to anode or cathode kinetics. In order to estimate the contribution of each electrode side, we performed impedance measurements in symmetrical cell mode at open cell voltage. Fig. 5 shows a Bode diagram for a symmetrical cell H_3PO_4/PBI-5N SiO_2-Im composite membrane. For the anode impedance measurements both sides were fed with hydrogen, whereas to study the cathode behavior air/air gas feedings were used. In the low frequency region, the total cell impedance dramatically increases when changing from the hydrogen symmetrical cell mode to the air one. This result clearly showed that the cathode response dominated in the chosen frequency range whereas the anode overall contribution to the cell impedance is negligible. These results are in agreement with previous findings reported in the literature (see ref. [16] and references therein).

The Nyquist spectra of the MEAs were obtained at current densities in the range 50–300 mA cm^{-2}. All the spectra were fitted with the equivalent model proposed in [15] (see Fig. 4 inset). A detailed explanation of the physical meaning of the different passive elements included in the model is reported in [15,16]. In particular, R_m represents the membrane resistance and is given by the high-frequency intercept of the spectrum with the real axis. The low frequency arc intercept can be attributed to the sum of the charge transfer resistance, R_{ct}, of oxygen reduction reaction, ORR, and the mass transfer resistance of the gases, R_{mt}. As far as

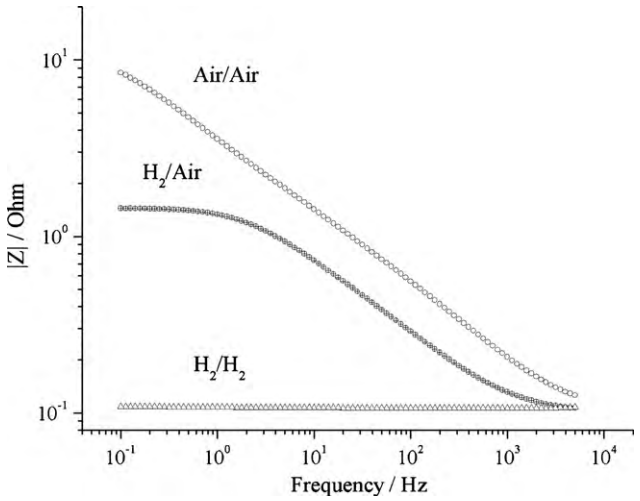

Fig. 5. Bode diagram of the PEMFC with H_3PO_4/PBI-5N composite membrane with 20 wt.% SiO_2-Im, at 150 °C, ambient pressure, symmetrical gas supply and 0% RH.

the membrane resistance is concerned, we obtained the values of $R_m = 0.1 \pm 0.02$, nearly independent of the membrane nature (with or without fillers) and the employed current density. This value is in reasonable agreement with that recently reported by Huth et al. [17]. Fig. 6 shows the behavior of the charge transfer resistance, R_{ct}, vs. the current density for the different membranes. In all the cases, R_{ct} decreases by increasing the current density, in agreement with the results reported in [15,16]. Our absolute values are 2–3 times higher, likely because our commercial electrodes are not optimized in terms of the overall composition and mainly, as far as it is concerned, the ionomer nature and content. In fact, the values reported in papers [15,16] were obtained on commercial MEAs, from PEMEAS and BASF respectively. The addition of both the fillers is beneficial, since it causes a substantial decrease in R_{ct} above 100 mA cm^{-2}, which is the reason of the increase in the maximum power density reported in Fig. 3. A more detailed study at different temperatures (now in progress) may help to understand the different behavior vs. temperature displayed in the *I–V* curves by SiO_2-Im and MCM-41. Finally, the values obtained for the mass transfer resistance, R_{mt}, lie in the range of 0.01–0.1 Ω cm^2, i.e. at least one order of magnitude lower than R_{ct}, without showing any clear trend. This is in agreement with the results of Zhang et al. [15], who showed that R_{mt} starts to increase above 0.1 Ω cm^2 for current densities higher than 1 A cm^{-2}. Jespersen et al. [16]

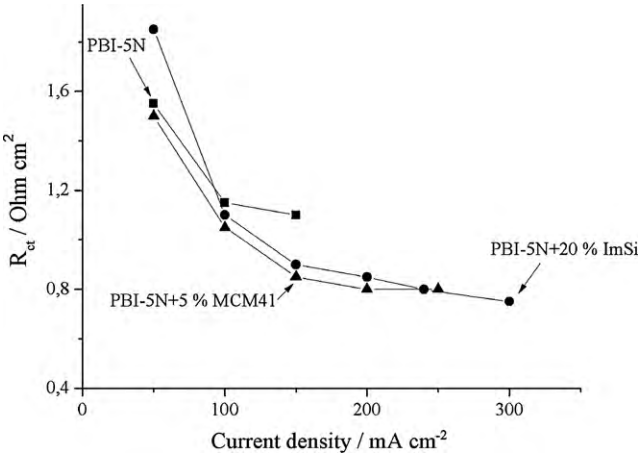

Fig. 6. Charge transfer resistance, R_{ct}, vs. the current density for the different membranes.

reported a nearly constant value of 0.2 $\Omega\,cm^2$ at 0.33 $A\,cm^{-2}$ for air stoichiometry $\lambda > 4$.

4. Conclusions

We prepared and tested PBI-based MEAs with and without fillers. A mesoporous filler, MCM-41, and a imidazole-functionalized one, SiO_2-Im, were used. The addition of the fillers increases the plateau of thermal stability of the PBI-5N membrane and it allows to obtain 20% higher maximum power densities compared to the pure PBI-5N MEAs. The SiO_2-Im filler is more effective than MCM-41 at temperatures above 120 °C.

The EIS technique showed that the fillers mainly help to reduce the charge transfer resistance of the cathodic side. The filler effects on the membrane resistance are negligible under the fuel cell operating conditions. The gas transfer resistance may be neglected with respect to R_{ct}, at least at low current densities.

Acknowledgment

This work was supported by the Cariplo Project "Development of new materials and demonstration of prototypes of polymer and solid oxide fuel cells".

References

[1] Q. Li, J.O. Jensen, R.F. Savinell, N.J. Bjerrum, Progress in Polymer Science 34 (2009) 449.
[2] J. Hu, H. Zhang, Y. Zhai, G. Liu, B. Yi, International Journal of Hydrogen Energy 31 (2006) 1855.
[3] P. Mustarelli, E. Quartarone, A. Magistris, in: J. Garche, et al. (Eds.), Encyclopedia of Electrochemical Power Sources, Elsevier, 2009, ISBN: 0-444-52093-7.
[4] S. Yu, L. Xiao, B.C. Benicewicz, Fuel Cells 3–4 (2008) 165.
[5] R. He, Q. Li, G. Xiao, N.J. Bjerrum, Journal of Membrane Science 226 (2003) 169.
[6] S.-W. Chuang, S.L.-C. Hsu, C.-L. Hsu, Journal of Power Sources 168 (2007) 172.
[7] M.-Q. Li, Z.-G. Shao, K. Scott, Journal of Power Sources 183 (2008) 69.
[8] M.Y. Jang, Y. Yamazaki, Journal of Power Sources 139 (2005) 2.
[9] Suryani, Y.-L. Liu, Journal of Membrane Science 332 (2009) 121.
[10] E. Quartarone, A. Magistris, P. Mustarelli, S. Grandi, A. Carollo, G.Z. Żukowska, J.E. Garbarczyk, J.L. Nowiński, C. Gerbaldi, S. Bodoardo, Fuel Cells 9 (2009) 349.
[11] A. Carollo, E. Quartarone, C. Tomasi, P. Mustarelli, F. Belotti, A. Magistris, F. Maestroni, M. Parachini, L. Garlaschelli, P.P. Righetti, Journal of Power Sources 160 (2006) 175.
[12] P. Mustarelli, E. Quartarone, S. Grandi, A. Carollo, A. Magistris, Advanced Materials 20 (2008) 1339.
[13] E. Caponetti, A. Minoja, M.L. Saladino, A. Spinella, Microporous and Mesoporous Materials 113 (2008) 490.
[14] S.R. Samms, S. Wasmus, R.F. Savinell, Journal of Electrochemical Society 143 (1996) 1225.
[15] J. Zhang, Y. Tang, C. Song, J. Zhang, Journal of Power Sources 172 (2007) 163.
[16] J.L. Jespersen, E. Schaltz, S.K. Kær, Journal of Power Sources 191 (2009) 289.
[17] A. Huth, B. Schaar, T. Oekermann, Electrochimica Acta 54 (2009) 2774.